SP-230—61

Shear Strength Prediction of Deep CFFT Beams

by I. Ahmad, Z. Zhu, A. Mirmiran, and A. Fam

Synopsis: Despite significant theoretical advances in the use of concrete-filled fiber reinforced polymer (FRP) tubes (CFFT), research on their shear behavior has been few and limited. Current method of shear analysis of CFFT beams relies on Bernoulli beam theory, which utilizes the basic assumption of linear strain distribution across the depth. Most recently, the use of modified compression field theory was suggested to improve the shear analysis of CFFT beams. The approach, however, is not applicable to the disturbed or D-regions of a beam, such as those in a deep CFFT beam. Therefore, this study adopted the strut-and-tie model to predict the shear strength of deep CFFT beams. The model is validated against test results for a CFFT beam with a shear-span-to-depth ratio of 1. A parametric study is then carried out to assess the shear criticality of CFFT beams. The study showed that shear failure would only be critical for beams with shear span less than their depth. High strength concrete was also found to improve capacity of CFFT beams. However, a judicious selection of concrete strength and fiber architecture with different proportions of shear and flexural capacities of the tube could help optimize the use of materials.

Keywords: concrete; deep beam; FRP; shear; strut-and-tie model

Iftekhar Ahmad received his Ph.D. degree in structural engineering and mechanics from North Carolina State University in Raleigh, NC in December 2004. He is currently employed as a structural engineer at ONM&J Inc., West Palm Beach, FL. His primary research interests are shear behavior of composite members, strut-and-tie model, fatigue in bridge members, and FRP applications in structural rehabilitation.

ACI Member **Zhenyu Zhu** received his Ph.D. degree from North Carolina State University in Raleigh, NC in December 2004. He is currently a Research Associate at Florida International University in Miami, FL. He is an associate member of committee 440. His research interests include construction issues and seismic behavior of hybrid concrete-FRP structures, and FRP applications in structural rehabilitation.

ACI Member **Amir Mirmiran** is Professor and Chair of the Department of Civil and Environmental Engineering at Florida International University in Miami, FL. He is a voting member of Committee 440, and Co-Chair of Subcommittee 440-J Stay-in-Place FRP Forms. His research interests include the use of advanced composites in infrastructure.

ACI Member **Amir Fam** is Assistant Professor and Canada Research Chair in Innovative and Retrofitted Structures at Queen's University, Canada. He is a voting member of Committee 440, FRP Reinforcement and Co-Chair of Sub-committee 440-J, Stay-in-Place Formwork. His research interests include applications of FRP in new construction and retrofit of existing structures.

INTRODUCTION

Use of fiber reinforced polymer (FRP) composites has recently gained wide acceptance as an economical technique for strengthening and rehabilitation of existing concrete structures. Thriving incorporation of FRP in retrofit measures has led to the development of an innovative hybrid construction concept and system (Mirmiran and Shahawy 1995) that utilizes FRP tube and concrete as the two basic materials for member design. Basic role of FRP tube in this system is to replace steel, while concrete serves the same purpose as that in conventional reinforced concrete structures. In addition, FRP tube renders itself as permanent formwork, protective jacket, confinement, shear and flexural reinforcement, whereas concrete provides the compressive strength for the member and stability for the tube against lateral buckling. The composite system thus formed is commonly referred to as concrete-filled FRP tubes (CFFT), and is found a viable alternative to reinforced or prestressed concrete for use as columns, piles and beams (Karbhari et al. 2000, Mirmiran 2003, Mirmiran and Shahawy 2003).

In the last decade, considerable research effort has been directed towards characterizing the CFFT system under axial compression (Samaan et al. 1998, Fam and Rizkalla 2001), flexural and axial-flexural loading (Mirmiran et al. 2000, Davol et al. 2001, Fam and Rizkalla 2002), simulated seismic loading (Shao et al. 2005, Zhu 2004), as well as long-term sustained loading (Naguib and Mirmiran 2001 and 2002). Superior performances, comparable to reinforced and prestressed concrete, have been documented

for CFFT members under static and pseudo-static loading. In the modeling arena, significant work has been carried out to better understand the behavior of the CFFT system, and subsequently establish necessary design guidelines for practical implementation. However, a detailed review of literature indicates that response under short-term static shear loading has received little or no attention (Burgueno and Bhide 2004). It is evident that in real applications the CFFT system will be subjected to shear forces in addition to other types of loading. Therefore, the increasing use of CFFT system in infrastructure will depend on better understanding of the shear resistance of CFFT, which in turn depends on the development of proper analytical tools that address responses under all primary load demands including shear.

A study was undertaken to address the shear behavior and strength predication of CFFT beams. The study consisted of two phases namely; experimental and analytical. This paper reports on the analytical modeling. The model aims at predicting the capacity of deep CFFT beams based on the well known strut-and-tie approach. The experimental phase has been reported elsewhere (Ahmad 2004). However, a brief summary of shear tests is included herein to provide instant reference to the reader.

SUMMARY OF TEST PROGRAM

A total of 10 CFFT beams were tested as a part of the experimental program. The test program was developed in conjunction with two previous research projects by Mirmiran et al. (2000) and Fam and Rizkalla (2002) mainly to cover a wide range of a/D_o, where a is the shear span and D_o is the outside diameter of the tube. Mirmiran et al. (2000) conducted flexure tests on short beams, using two different tubes of type I and II, as shown in Table 1. Beams S-3 and S-6 had a/D_o ratios of 1.93 and 2.04 respectively. Similar GFRP tubes were used to fabricate the companion deep CFFT beams. Fam and Rizkalla (2002) investigated flexural behavior of slender CFFT beams S-7 and S-8 with types III and IV tubes respectively and a/D_o ratios in excess of 6. In fact, the deep beams S-7 and S-9 were cast as a part of the experimental program of Fam and Rizkalla (2002). Some of the specimens for this project were cut from the same long span beams. Irrespective of the tube types and a/D_o ratios, all beams tested previously had failed in flexure including the lowest a/D_o ratio of 1.92. Hence, the a/D_o ratio of 1 was selected and companion deep beams were tested to identify the shear criticality and failure modes of beams made with types I-IV tubes. Parameters studied included effect of fiber architecture, a/D_o ratio, reinforcement index, and diameter-to-thickness ratio of the tube. Figure 1 depicts a typical view of the test setup. Table 2 shows the details of the tested beams. Test results enhanced the data base of CFFT beams to the lowest practical value of a/D_o ratio of 1. Test results also enlightened the fact that shear may not be a critical issue for CFFT beams when compared with their RC counterparts for a/D_o ratios as low as 1.

STRUT-AND-TIE MODEL FOR DEEP CFFT BEAMS

Although significant modeling efforts have been reported on the axial and flexural behavior of CFFT members, none is directly applicable to deep CFFT beams. Bhide (2002) and Burgueno and Bhide (2004) have recently augmented the modified compression field theory (MCFT) with the classical lamination theory (CLT) to model shear response of CFFT beams. The approach is based on a sectional layered analysis with an iterative algorithm to achieve equilibrium and compatibility conditions for the composite system, including the cracked behavior of the FRP-confined concrete and the first-ply-failure criterion for the FRP tube. The model assumes linear strain distribution across the depth, and resolves the shear stress distribution from the first order mechanics. However, it is important to note that the model is applicable only to the so-called B-region, where Bernoulli's beam theory applies. In the disturbed or D-region, such as CFFT beams with a/D_o ratio of 1, inherent assumptions in the model do not apply, since the behavior is dominated by the arching action rather than the beam bending action. Hence, the model tends to provide lower bound strengths for short and deep CFFT beams.

Previous attempts at estimating shear capacity of CFFT beams also include modifications by Seible et al. (1996) of the UCSD shear strength model developed at the University of California, San Diego by Priestley et al. (1993) for RC members. In their model, shear strength V_n consists of two components, similar to the shear equation of the ACI 318-02 (2002), as given by

$$V_n = V_c + V_j \tag{1}$$

where V_c is concrete's contribution, which is based on ductility of the member, as expressed by

$$V_c = \gamma \sqrt{f_c'}\, 0.8\, A_g \tag{2}$$

where γ accounts for the reduced shear resisting mechanism of concrete with the higher ductility, and ranges between 0.1 and 0.29, and A_g is the gross area of concrete section. The truss component V_j was developed for a 45° angle between the compression diagonal and the axis of the member, taking into account the effect of multiple angle plies, as given by

$$V_j = \sum_{i=1}^{n_w} \frac{\pi}{2} D_o\, t_j\, f_{45^o \pm \theta_i} \tag{3}$$

where n_w is the total number of winding angles, D_o is the outer diameter of the tube, t_j is the lamina thickness for each winding angle, and $f_{45^o \pm \theta i}$ is the ultimate tensile strength at the winding angle θ_i. Since the equation adopts 45° crack angle, it implies that compressive stress trajectories are uniform, and thereby assumes the entire length of the member as a B-region. However, the actual internal flow of forces in a disturbed or D-

region could be significantly different. It is therefore necessary to use a procedure that more closely represents the actual flow of forces.

Strut-and-tie truss model or the load path method has been shown to closely model internal force flow in a D-region of a deep RC beam(Schlaich et al. 1987). Furthermore, the empirical Equation (2) or the comparable ACI equation may underestimate the shear contribution of concrete, V_c in deep beams by as much as 2-3 times. Also, Equation (3) does not take into account the interaction between the lamina layers and the principal stress components. Therefore, the predicted V_j could be higher than what an angle ply laminate can actually resist.

According to St. Venant's principle (Schlaich et al. 1987), D-regions are generally located within a length equal to the beam depth D_o from the support and the load point. For a deep CFFT beam with a/D_o of 1, the entire beam can be regarded as highly disturbed with overlapping D-regions and non-linear strain distribution. As shown in Figure 2, a rigorous strut and tie model was developed in lieu of a simple truss. The model comprises of multiple struts and a connecting tie.

Tests data (Rogowsky and Macgregor 1986) have shown that shear strength of a deep RC beam increases with lower shear-span-to-depth ratio because of the direct compression strut between the load and the support. Subsequently, the slope of the major compression diagonal strut is an important parameter, and is better defined by the a/D_o ratio. Following a similar format of the ACI shear equation, the shear force in a deep CFFT beam is proposed to consist of two components of V_c and V_j, where the former accounts for the direct shear transfer in the major compression strut between the load and the support, and the latter stems from truss mechanism of the compression fan like struts of concrete and FRP. These struts at the load and reaction points provide stability to the tube under lateral buckling. Figures 3 and 4 show the details of internal force flow of the truss model. The proposed truss model is highly indeterminate in nature. Geometry of the compressive struts is established by keeping the strut angles between 25^o and 65^o. Number of the struts varies depending on the length of the shear span. Two or three iterations may be required before the geometry of the truss is finalized. The following assumptions are made for the analysis:

1) Failure of the tube takes place at 45^o angle, which is on the plane joining the load and the support for a beam with a/D_o ratio of 1. This is confirmed by test observations that the principal tensile strain at mid-depth coincides with strain reading at 45^o (see Ahmad 2004).
2) Effective length of the tube for resisting shear is the length between the compression fan like struts that contribute V_j to the total shear force (see Figure 2).
3) Vertical component of FRP diagonal shear is equally distributed to the nodes of the truss that consists of compression fan like struts and the tube. This assumption is similar to the yielding of all stirrups in an RC deep beam.
4) Perfect bond and full composite action are assumed between concrete and FRP tube, so that there will be no slippage. End plate of the tension tie simulates the

embedment of FRP tube in adjacent members, which is the case in structural applications.

Figure 4 illustrates the force equilibrium of the truss system and the nodes. It is assumed that the horizontal force in concrete at the support node is fully transferred to the tube by mechanical friction. For partial composite action, the strut force induced in concrete depends on the friction force imparted by the interface. Once the bond strength is estimated, concrete strut force can be calculated by force transformation. Irrespective of the composite action, support reaction will significantly enhance the frictional resistance by bearing.

Several reasonable assumptions were made to allow for sizing of the compressive struts and tension tie, and determining their stresses. Flexural analysis of CFFT beam suggests that that the neutral axis is located within a region of $0.2 \sim 0.4D_o$. Depth of the C-C-C node that is subjected to compressive force was therefore assumed to be $0.3D_o$. Unlike an RC beam, reinforcement in CFFT beams is distributed throughout the depth. Observation of failure modes of deep CFFT beams indicates that cracks propagated up to mid-depth of the member at failure. Therefore, the bottom half of the tube was considered effective in resisting tension at mid-span. Tensile and compressive stress distributions are assumed linear above and below the CCC node. An equivalent rectangular stress block is assumed for concrete compressive stress at mid-span. Equilibrium of forces can then be written as

$$C_h + C_{fh} = T_f \tag{4}$$

where T_f is the tensile force in the bottom half of FRP tube, C_h is the horizontal component of compressive strut in concrete, and C_{fh} is the induced compressive force in the FRP tube due to compression fan like struts radiating from the load point. Based on the strut and tie model, three types of failure mode could be identified, as follows: (a) shear failure (rupture of the FRP tube under diagonal tension, or crushing of any compression strut, or combined failure of FRP and any compression strut), (b) flexural failure (rupture of tension tie at the bottom in mid-span) or (c) bearing failure at the C-C-C node (load point) or C-C-T node (reaction point) under excessive bearing stresses. The truss element that has the weakest capacity in the induced loading direction will govern the overall failure mode of the beam. From the free body diagram, failure load is the smaller of the shear and flexural resistance, as given by

$$P_u = 2\left(V_C + V_j\right) \tag{5}$$

$$P_u = \frac{2\ \alpha\ D_o\ T_f}{a} \tag{6}$$

where αD_o is the lever arm between compression and tension forces, and T_f is tie force given by

$$T_f = \frac{\pi t_j}{2}\left(D_o - t_j\right)\frac{1.29\, f_{fu}}{2} \tag{7}$$

where f_{fu} is the ultimate tensile strength of FRP. T_f is acting at the centroid of the bottom half of the tube. Figure 5 depicts the qualitative shape of the compressive strut. ACI 318-02 (2002) and AASHTO LRFD (1998) suggest the effective width of a circular section to be D_o for calculation of V_c. Here, a conservative width of $0.8D_i$ (see Figure 5) is taken as the effective width of the strut, where D_i is the concrete core diameter. Once the load bearing plate dimensions are known, strut width could be established. Effective compressive strength f_{ce} in concrete strut is adopted from Macgregor (1997), as given by

$$f_{ce} = \nu_1\, \nu_2\, f_c^{'} \tag{8}$$

where v_1 and v_2 are the efficiency factors, with v_1 selected as 0.8 for CFFT beams based on the values given for deep RC beams in the same reference, and v_2 is given as

$$\nu_2 = 0.55 + \frac{15}{\sqrt{f_c^{'}}} \quad (f_c^{'} \text{ in psi}) \tag{9a}$$

$$\nu_2 = 0.55 + \frac{1.25}{\sqrt{f_c^{'}}} \quad (f_c^{'} \text{ in MPa}) \tag{9b}$$

The required strut thickness is calculated once the effective compressive strength f_{ce} is known. Recommended stresses in C-C-C and C-C-T nodal zones are $0.85\, f_c^{'}$ and $0.75\, f_c^{'}$, respectively, as per the ASCE-ACI Committee (1998) on shear and torsion.

MODEL VALIDATION

For brevity, typical verification of the above model is discussed here for beam S-9. In a typical RC beam, about 25%-40% of the shear force is carried by stirrups to ensure ductile mode of failure (Macgregor 1997). However, in majority of CFFT beams the effective amount of shear reinforcement is much greater than RC beams due to the continuous form of shear reinforcement over the shear span. Therefore, it may be reasonable to start with a value of 50% of the total shear transferred through truss mechanism. Tables 3 and 4 show the lamina thickness and properties of the GFRP tube used to fabricate beam S-9. Laminate analysis was performed to obtain the strength of the laminate, f_{fu} perpendicular to the failure plane. Progressive laminate failure analysis (Daniel and Ishai 1994) was carried out with Tsai-Wu failure criteria (Daniel and Ishai 1994) for laminate, and strength was found to be 16.82 ksi (116 MPa) for tube type IV. Failure plane was assumed at 45^o angle, as confirmed by the tests. After finalizing the

truss geometry, ultimate load P_u was found to be 178 kips (792 kN) and 202 kips (898.5 kN) to fail the beam S-9 in flexure and shear, respectively. This indicates that flexure governs the mode of failure, as confirmed by the tests. The predicted failure load also agrees favorably with the experimental load of 190 kips (845 kN). The analysis showed that shear failure, if critical, would occur by crushing of the struts BH and AB (see Figure 3) rather than diagonal tension failure of the tube. Stresses in nodes C-C-C and C-C-T were both below the respective limiting stresses.

PARAMETRIC STUDIES ON SHEAR CRITICALITY

The above strut-and-tie model was used to evaluate the shear criticality of CFFT beams in a parametric study with the following four key factors: (a) fiber architecture, (b) a/D_o ratio, (c) D_o/t_j ratio, and (d) concrete strength, f_c'. For simplicity and practicality, all material and geometric properties were selected to vary around those of beam S-9 described above in the model validation, unless otherwise noted.

Figure 6 shows the effect of fiber architecture on the ratio of the ultimate load P_u for shear to its value under flexure. The ratio indicates shear criticality, if less than 1. The fiber architecture is taken as a parameter, since it also reflects the effect of jacket strength, f_j in the axial and hoop directions and the fiber volume fraction of the laminate. Three types of laminate architecture were used to study the effect of this factor on shear criticality. Type of angle ply has the same lay-up, thickness, and materials as tube type IV and can be regarded as the intermediate case. Types of axial and hoop represent two extreme cases of 0^o and 90^o angles, respectively, or in other words, the least shear capacity and the least flexural capacity, respectively. They both fail by splitting of the tube parallel to the fiber direction. The figure clearly shows that axial fiber orientation, such as in pultruded shapes, is vulnerable to horizontal shear failure. On the other hand, angle plies are generally better in terms of shear capacity, and can be optimized for a balanced design of flexure and shear.

Figure 7 depicts the effect of a/D_o ratio on shear criticality of CFFT beams. As the a/D_o ratio approaches 0.5, the number of struts consolidates to only one major diagonal strut. However, for a/D_o of 0.75, the number of compression fan like struts reduces to two. Due to lack of any experimental evidence, a 45^o angle can be assumed for tubes all cases, even though it is believed that it may be somewhat higher for the a/D_o ratio of 0.75. Analysis reveals that for the a/D_o ratio of 0.5, shear contribution of concrete is about 100% of the total capacity due to the increase in major compression strut angle and a decrease in the effective length of the tube. For higher values of a/D_o ratio, if a beam is sufficiently slender so that compression fan regions at the load and reaction points do not overlap, no major compression strut will exist. Instead, a uniform compression stress field will develop, which means that the method proposed by Burgueno and Bhide (2004) would be appropriate. However, a truss model can also be developed to predict the shear capacity of slender CFFT beam. It can be seen from the figure that critical a/D_o ratio is about 0.9 for this particular set of parameters.

Figures 8 and 9 show the effects of D_o/t_j ratio and concrete strength, respectively, on shear criticality of CFFT beams. The D_o/t_j ratio is varied by changing the thickness of lamina layers of tube type IV. Both parameters show similar trends as that for the a/D_o ratio. Shear tends to be critical for very low values of each parameter. Flexural capacity is more sensitive to the D_o/t_j ratio, while shear capacity is more sensitive to concrete strength.

A careful observation of the effect of concrete strength reveals important aspects of shear design of CFFT beams. At lower levels of concrete strength, a brittle shear failure may occur in one or more concrete struts, while at higher levels of concrete strength, a combined failure of concrete struts and FRP tube may take place with some ductility imparted from the FRP tube. Therefore, a higher concrete strength is generally more desirable. A judicious selection of concrete strength and fiber architecture with different proportions of shear and flexural capacities of the tube can help optimize the use of materials.

SUMMARY AND CONCLUSIONS

Despite significant theoretical advances on the axial and flexural behavior of concrete-filled fiber reinforced polymer (FRP) tubes (CFFT), research on their shear behavior has been few and limited. Most recently, the use of modified compression field theory was suggested to model shear response of CFFT beams. The approach, however, is not applicable to the disturbed or D-regions of a beam, such as those in a deep CFFT beam. Therefore, this study adopted the strut-and-tie model to predict the shear strength of deep CFFT beams. The model was validated against test results for a CFFT beam with a shear-span-to-depth ratio of 1. Predictions showed good agreement with test results. A parametric study was then carried out to assess the shear criticality of CFFT beams. It was concluded that shear failure would only be critical for beams with shear span less than their depth. High strength concrete was found to improve capacity of CFFT beams. However, a judicious selection of concrete strength and fiber architecture with different proportions of shear and flexural capacities of the tube could help optimize the use of materials.

ACKNOWLEDGMENTS

Financial support for this study was provided by the National Science Foundation as part of the Faculty Career Award to Dr. Mirmiran. Additional support was provided by the Florida Department of Transportation. However, views and opinions expressed in this paper are those of the authors alone and not necessarily those of the sponsoring agencies.

REFERENCES

AASHTO, (1998) *AASHTO-LRFD Bridge Design Specifications*, AASHTO, 2nd Ed., Washington, DC, 1091 p.

ACI Committee 318, (2002) *Building Code Requirements for Structural Concrete and Commentary*, ACI, Farmington Hills, MI, 443 p.

Ahmad, I., (2004) "Shear Response and Bending Fatigue Behavior of Concrete-Filled Fiber Reinforced Polymer Tubes," *Ph.D. Thesis*, North Carolina State University, Raleigh, NC, 195 p.

ASCE-ACI Committee, (1998) "Recent Approaches to Shear Design of Structural Concrete," *Journal of Structural Engineering*, V. 124, No. 12, pp. 1375-1417.

Bhide, K., (2002) "Shear Response of Concrete-Filled Circular Fiber-Reinforced Polymer Composite Tubes," *M.S. Thesis*, Michigan State University, East Lansing, MI, 109 p.

Burgueno, R., and Bhide, K., (2004) "Shear Stresses in Concrete-Filled FRP Cylindrical Shells in Bending," *Proceedings of the 4th Advanced Composite Materials in Bridges and Structures*, Calgary, Canada, pp. 1-8.

Daniel, I., and Ishai, O., (1994) *Engineering Mechanics of Composite Materials*, Oxford University Press, 395 p.

Davol, A., Burgueno, R., and Seible, F., (2001) "Flexural Behavior of Circular Concrete Filled FRP Shells," *Journal of Structural Engineering*, ASCE, V. 127, No. 7, pp. 810-817.

Fam, A., and Rizkalla, S., (2001) "Confinement Model for Axially Loaded Concrete Confined by Circular Fiber-Reinforced Polymer Tubes," *ACI Structural Journal*, V. 98, No. 4, pp. 451-461.

Fam, A., and Rizkalla, S., (2002) "Flexural Behavior of Concrete-Filled Fiber-Reinforced Polymer Circular Tubes," *Journal of Composites for Construction*, ASCE, V. 6, No. 2, pp. 123-132.

Karbhari, V., Seible, F., Burgueno R., Davol, A., Wernli, M., and Zhao, L., (2000) "Structural Characterization of Fiber-Reinforced Composite Short-and Medium-Span Bridge Systems," *Applied Composite Materials*, V. 7, pp. 151-182.

Macgregor, J., (1997) *Reinforced Concrete – Mechanics and Design*, Prentice-Hall Inc., 3rd Ed., 937 p.

Mirmiran, A., (2003) "Stay-In-Place Form for Concrete Columns," *Advances in Structural Engineering*, V. 6, No. 3, pp. 231-241.

Mirmiran, A., and Shahawy, M., (1995) "A Novel FRP-Concrete Composite Construction for the Infrastructure," *Proceedings of Structures Congress XIII*, ASCE, Boston, MA, pp. 1663-1666.

Mirmiran, A., and Shahawy, M., (2003) "Composite Pile: A Successful Drive," *Concrete International*, V. 25, No. 3, pp. 89-94.

Mirmiran, A., Shahawy, M., El Khoury, C., and Naguib, W., (2000) "Large Beam-Column Tests on Concrete-Filled Composite Tubes," *ACI Structural Journal*, V. 97, No. 2, pp. 268-276.

Naguib, W., and Mirmiran, A., (2001) "Time Dependent Behavior of FRP-confined Concrete Columns: Experiments and Modeling, "*ACI Structural Journal*, V. 99, No. 2, pp. 142-148.

Naquib, W., and Mirmiran, A., (2002) "Flexural Creep Tests and Modeling of Concrete-Filled Fiber Reinforced Polymer Tubes," *Journal of Composites for Construction*, ASCE, V. 6, No. 4, pp. 272-279.

Priestley, M., Verma, R., and Xiao, Y., (1993) "Seismic Shear Strength of Reinforced Concrete Columns," *Journal of Structural Engineering*, ASCE, V. 120, No. 8, pp. 2310-2329.

Rogowsky, D., and Macgregor, G., (1986) "Design of Reinforced Concrete Deep Beams," *Concrete International*, ACI, V. 8, No. 8, pp. 49-58.

Samaan, M., Mirmiran, A., and Shahawy, M. (1998) "Model of Concrete Confined by Fiber Composites," *Journal of Structural Engineering,* ASCE, V. 124, No. 9, pp. 1025-1031.

Schlaich, J., Schafer, K., and Jennewein, M., (1987) "Toward a Consistent Design of Structural Concrete," *PCI Journal,* Prestressed Concrete Institute, V. 32, No. 3, pp. 74-150.

Seible, F., Burgueno, R., Abdallah, M., and Nuismer, R., (1996) "Advanced Composite Carbon Shell Systems for Bridge Columns under Seismic Loads," *Proceedings of the 11th World Conf. Earthquake Engineering*, Elsevier Science, Oxford, Paper No. 1375.

Shao, Y., Aval, S., and Mirmiran, A., (2005) "Fiber-Element Model for Cyclic Analysis of Concrete-Filled Fiber Reinforced Polymer Tubes," *Journal of Structural Engineering*, ASCE, V. 131, No. 2, pp. 292-303.

Zhu, Z., (2004) "Joint Construction and Seismic Performance of Concrete Filled Fiber Reinforced Polymer Tubes," *Ph.D. Thesis*, North Carolina State University, Raleigh, NC, 215 p.

Table 1 - Mechanical properties of GFRP tubes used in CFFT beam shear tests

Tube type (Designated surface color)	Fiber architecture	Tensile strength ksi (MPa)	Tensile elastic modulus ksi (GPa)	Compressive strength ksi (MPa)	Compressive elastic modulus ksi (GPa)	Hoop strength ksi (MPa)	Hoop elastic modulus ksi (MPa)
I (Yellow)	$[\pm 55^{o}]$ 17 layers V_f= 75.5%	10.3 (71)	1820 (12.5)	33.3 (229.5)	1260 (8.7)	34 (234.5)	2000 (13.8)
II (White)	$[0^{o}/0^{o}/+45^{o}/-45^{o}]_{10}$ 40 layers V_f= 51.2%	57.9 (400)	2257 (15.5)	55.8 (384.5)	3375 (23.5)	N/A	N/A
III (Grey)	$[\pm 34^{o}+80^{o}\pm 34^{o}]$ 5 layers V_f= 51%	25.8† (178)	2132† (14.5)	34.5* (238)	N/A	19.0* (131)	1305* (9.0)
IV (Red)	$[\{-88^{o}+3^{o}-88^{o}\}_2$ $\{+3^{o}\}_1$ $\{-88^{o}+3^{o}-88^{o}\}_1]$ 10 layers V_f= 51%	34.4† (237)	2465† (17)	49.7* (343)	N/A	58.3* (402)	2857* (19.5)

* Predicted by laminate theory;
† Coupon testing by Fam & Rizkalla (2002)

Table 2 - Test matrix for slender, short and deep CFFT beams

Tube type	Beam No.	Outer dia., D_o in (mm)	Thickness t_j in (mm)	Span length, L in (mm)	Span-to-depth ratio, a/D_o	Concrete strength, f_c' ksi (MPa)	Beam type
I	S-1	12.68 (322.0)	0.200 (5.10)	22.8 (579)	0.9	5.9 (40.5)	Deep
	S-2	6.64 (168.6)	0.135 (3.43)	13.3 (338.0)	1.0		Deep
	S-3†	14.52 (368.8)	0.258 (6.60)	90.0 (2286)	1.93	3.4 (23.5)	Short
	S-4†	12.68 (322.0)	0.200 (5.10)	72.0 (1829)	1.89	4.5 (31.0)	Short
II	S-5	12.0 (305.0)	0.750 (19.00)	24.0 (610)	1.0	7.3 (50.5)	Deep
	S-6†	13.69 (347.7)	0.550 (13.90)	90.0 (2286)	2.04	4.2 (29.0)	Short
III	S-7	12.56 (319)	0.278 (7.10)	25.2 (640.0)	1	9.7 (67)	Deep
	S-8†			216.5 (5500)	6.25		Slender
IV	S-9	12.83 (326)	0.284 (7.20)	25.7 (653)	1	5.9 (40.5)	Deep
	S-10†			216.5 (5500)	6.14	8.7 (60)	Slender

† four point loading
Beam S-3 and S-6 : Mirmiran et al. (2000); Beam S-8 and S-10 : Fam and Rizkalla (2002)

Table 3 - Details of laminate architecture

Properties	Tube type IV									
Ply lay-up	-88	+3	-88	-88	+3	-88	+3	-88	+3	-88
Thickness in (mm)	0.022 (0.56)	0.017 (0.43)	0.022 (0.56)	0.022 (0.56)	0.035 (0.89)	0.022 (0.56)	0.034 (0.86)	0.022 (0.56)	0.034 (0.86)	0.022 (0.56)

Table 4 - Lamina properties for parametric study

Properties*	Values
E_1	5,511 ksi (38 GPa)
E_2	1,131 ksi (7.8 GPa)
G_{12}	507 ksi (3495 MPa)
v_{12}	0.28
F_{1t}	115.3 ksi (795 MPa)
F_{1c}	77.3 ksi (533 MPa)
F_{2t}	5.66 ksi (39 MPa)
F_{2c}	18.56 ksi (128 MPa)
F_6	12.91 ksi (89 MPa)

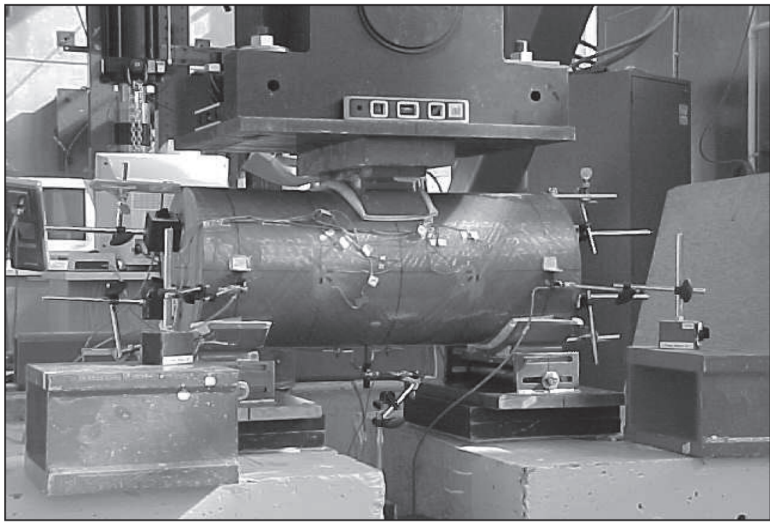

Figure 1—An overview of shear test setup

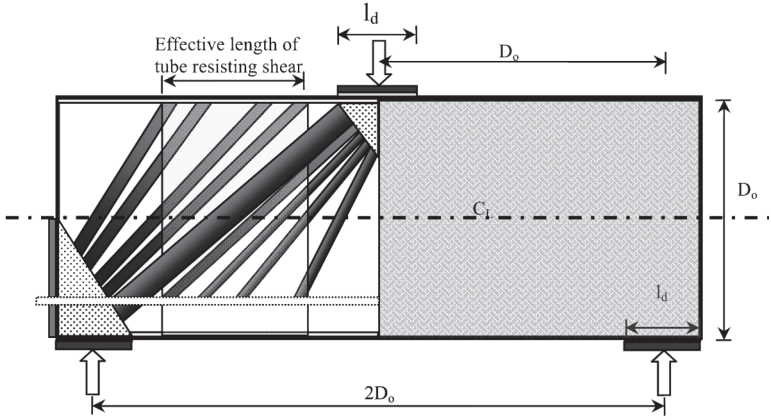

Figure 2 —Strut-and-tie model for deep CFFT beams

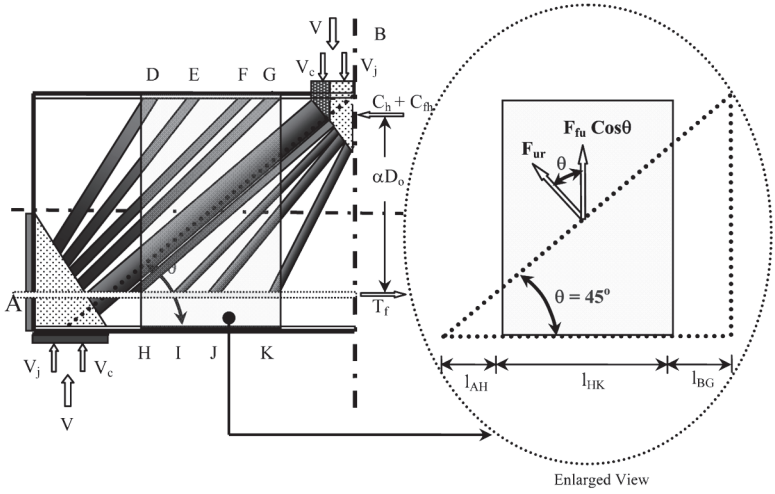

Figure 3—Details of strut-and-tie model

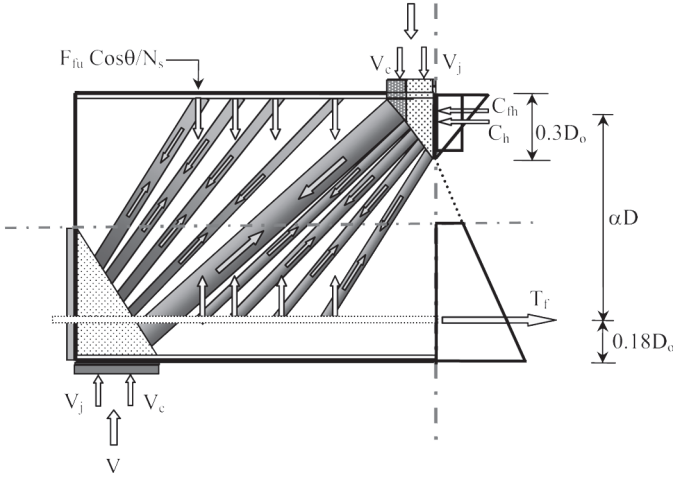

Figure 4—Equilibrium of truss model with internal force flow

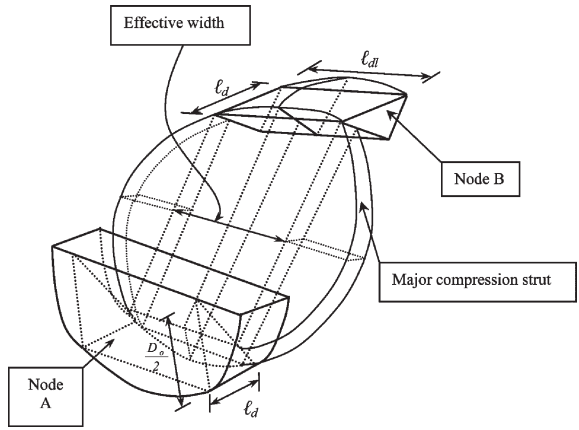

Figure 5—Qualitative shape of major compression strut

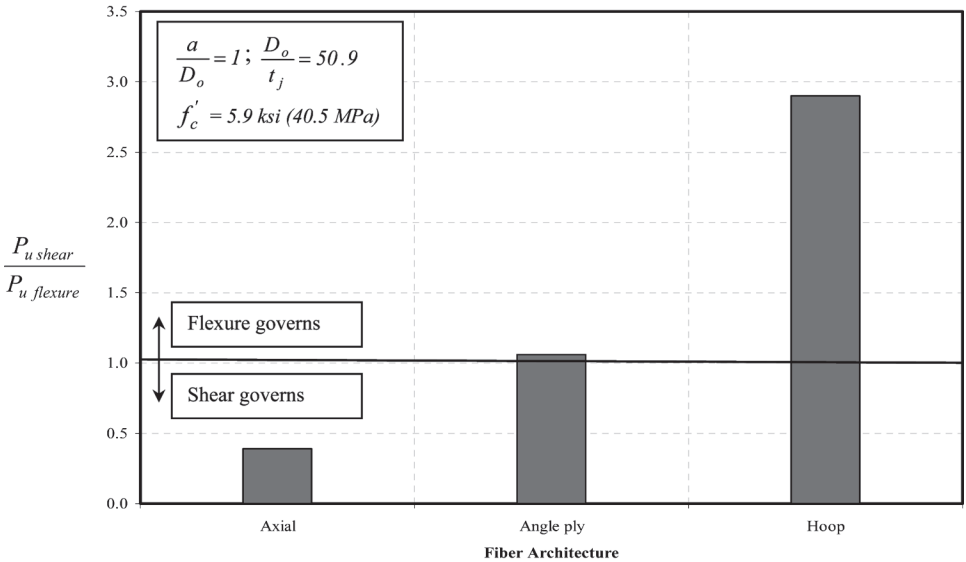

Figure 6—Effect of fiber architecture on shear criticality of CFFT beams

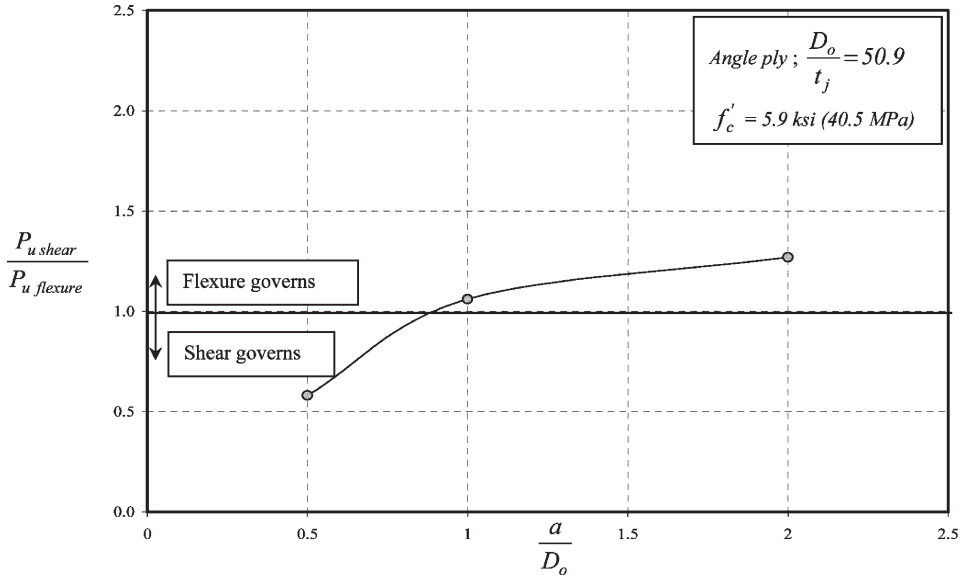

Figure 7—Effect of a/D_o ratio on shear criticality of CFFT beams

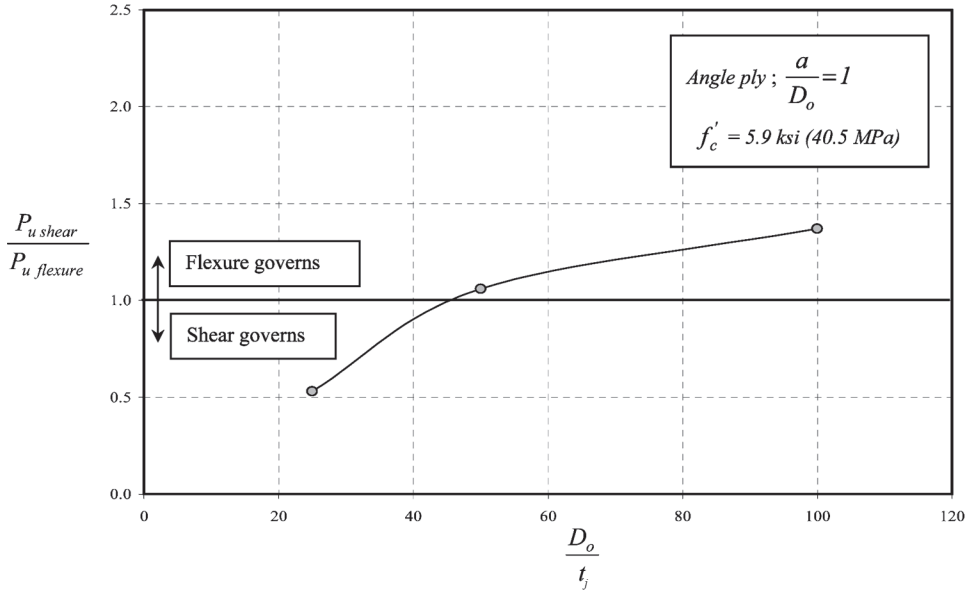

Figure 8—Effect of D_o/t_j ratio on shear criticality of CFFT beams

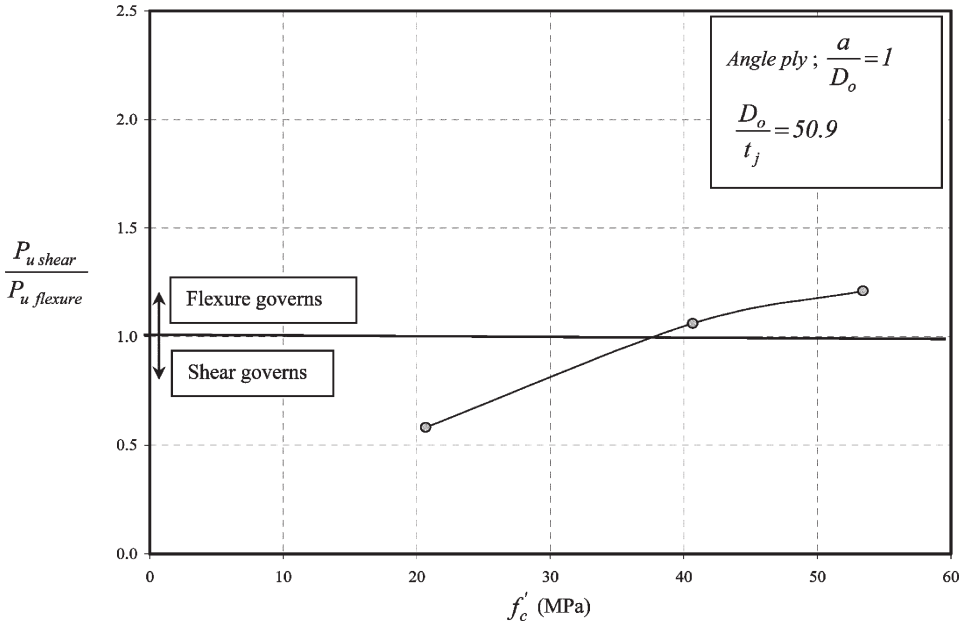

Figure 9—Effect of concrete compressive strength $f_c^{'}$ on shear criticality of CFFT beams